



Published in final edited form as:

Ann Plast Surg. 2013 February ; 70(2): 149–153. doi:10.1097/SAP.0b013e31822f9af7.

Quantitative Assessment of Nipple Perfusion with Near-Infrared Fluorescence Imaging

Yoshitomo Ashitate, M.D.^{1,2,*}, Bernard T. Lee, M.D., FACS^{3,*}, Long H. Ngo, Ph.D.⁴, Rita G. Laurence, B.S.¹, Merlijn Hutteman, M.Sc.^{1,5}, Rafiou Oketokoun, M.S.¹, Elaine Lunsford, B.S.¹, Hak Soo Choi, Ph.D.¹, and John V. Frangioni, M.D., Ph.D.^{1,6}

¹Division of Hematology/Oncology, Department of Medicine, Beth Israel Deaconess Medical Center, Boston, MA 02215 ²Division of Cancer Diagnostics and Therapeutics, Hokkaido University Graduate School of Medicine, Sapporo, Japan ³Division of Plastic and Reconstructive Surgery, Department of Surgery, Beth Israel Deaconess Medical Center, Boston, MA 02215 ⁴Division of General Medicine and Primary Care, Department of Medicine, Beth Israel Deaconess Medical Center, Boston, MA 02215 ⁵Department of Surgery, Leiden University Medical Center, Leiden, the Netherlands ⁶Department of Radiology, Beth Israel Deaconess Medical Center, Boston, MA 02215

Abstract

Preserving the nipple areolar complex with a nipple-sparing mastectomy improves cosmesis compared to skin-sparing mastectomy. However, complications such as necrosis of the nipple areolar complex significantly impact cosmetic outcome. Many factors influence nipple areolar perfusion and no consensus currently exists on optimal incisional choice. This study evaluates 2 nipple sparing mastectomy incision models using near-infrared (NIR) fluorescence to assess perfusion quantitatively. The periareolar and radial incisions were compared with 2 control models in Yorkshire pigs (N = 6). Methylene blue (MB) and indocyanine green (ICG) were injected intravenously and NIR fluorescence images were recorded at 3 time points: before surgery, immediately after (0 h), and 3 d postoperatively. Contrast-to-background ratio (CBR) was used to assess perfusion. At 72 h, radial incisions showed a statistically significantly higher perfusion compared to periareolar incisions ($P < 0.05$). Based on our findings, radial incisions for nipple sparing mastectomy may be preferable due to higher perfusion, however, clinical trials are necessary for further assessment.

Keywords

Nipple-sparing mastectomy; nipple areolar complex; periareolar incision; radial incision; indocyanine green; methylene blue; near-infrared fluorescence imaging

*To whom all correspondence should be addressed: John V. Frangioni, M.D., Ph.D., BIDMC, Room SL-B05, 330 Brookline Avenue, Boston, MA 02215, 617-667-0692 FAX: 617-667-0981, jfrangio@bidmc.harvard.edu.

*These authors contributed equally to this work.

FINANCIAL DISCLOSURE

All FLARE™ technology is owned by Beth Israel Deaconess Medical Center, a teaching hospital of Harvard Medical School. As inventor, Dr. Frangioni may someday receive royalties if products are commercialized. Dr. Frangioni is the founder and unpaid director of The FLARE Foundation, a non-profit organization focused on promoting the dissemination of medical imaging technology for research and clinical use.

INTRODUCTION

The use of nipple-sparing mastectomy has been slowly gaining acceptance in the United States. Despite initial concerns over indications and oncologic safety, large scale studies have shown similar rates of recurrence compared to skin-sparing mastectomy and a low rate of nipple areolar recurrences (1–5). Recent reports show that nipple sparing mastectomy is safe in prophylactic mastectomy, as 0% of nipples examined had occult disease compared to 21% of breasts after therapeutic mastectomy (6). Various studies have shown increased patient satisfaction after nipple sparing mastectomy and reconstruction due to the improved cosmetic outcome provided by preservation of the nipple areolar complex (7–9). Necrosis of the nipple areolar complex can be distressing to the patient who has elected to proceed with nipple sparing mastectomy. Previous reports in the literature show the incidence of partial necrosis is 1.0% to 23.5%, while the incidence of total necrosis is 0% to 9.6% (1, 7–19).

One major factor that contributes to the incidence of necrosis is the choice of incision. Selected incisions described in detail include periareolar, transareolar, inframammary, radial, and omega mastopexy incisions (10, 13, 16–19). However, there is no clear consensus in the literature as to which is the optimal incisional choice.

Near-infrared (NIR) imaging is a technology that combines low levels of safe, invisible NIR light with injection of a NIR fluorophore in order to highlight anatomical and/or functional features of interest during surgery. NIR light has several attractive features. It is invisible, so the look of the surgical field does not change. The technology is non-contact, with the imaging system typically 1 to 2 feet away from the patient. Unlike visible light, NIR light penetrates many millimeters into living tissue and is thus able to see blood vessels and other structures within and under the skin. Because many commercial and investigational NIR fluorescence imaging systems are already available (reviewed in (20)), much attention is now focused on developing NIR contrast agents for various clinical applications.

A key feature of NIR fluorescence is the ability to quantify metrics, such as perfusion, intraoperatively (21–24). Quantification of perfusion metrics allows one to correlate intraoperative NIR findings with clinical assessment postoperatively. The use of indocyanine green (ICG), an 800 nm NIR fluorophore FDA-approved for ophthalmic angiography, in conjunction with the FLARE™ imaging system has been previously described for perfusion assessment in perforator flaps (25). Methylene blue (MB) is a 700 nm NIR fluorophore that has been evaluated preclinically in cardiovascular surgery (26) and biliary tract surgery (27); however, it has not been extensively studied for assessment of skin perfusion. The current FDA approval for MB is for treatment of methemoglobinemia; however, it is routinely used during surgical procedures as a blue dye. After intravenous injection, MB is first-pass extracted by many tissues and organs, thus functioning as a perfusion tracer (26) whereas ICG remains extracellular. This property of MB may provide a unique advantage during perfusion assessment because its NIR fluorescence in skin is relatively stable and long-lived after a single intravenous injection.

In this study, a comparison between 2 common nipple-sparing mastectomy incisions has been performed in an animal model: a periareolar incision and a radial incision. The FLARE™ imaging system was used to assess quantitative perfusion metrics. Evaluation was performed with both MB and ICG to ascertain differences in perfusion and clinical outcome over a 72-hour period.

MATERIALS AND METHODS

Drugs, Chemicals, and *In Vitro* Optical Measurements

For quantitative assessment, the fluorophores selected were MB and ICG. MB was purchased from Taylor Pharmaceuticals (Decatur, IL). ICG was purchased from Akorn Inc., (Decatur, IL). All *in vitro* measurements were performed in 100% fetal bovine serum (FBS). Absorbance and fluorescence were measured with fiberoptic HR2000 absorbance (200–1100 nm) and USB2000FL fluorescence (350–1000 nm) spectrometers (Ocean Optics, Dunedin, FL). NIR excitation was provided by a 5-mW, 654-nm or a 250-mW, 770-nm laser diode. Fluorescence quantum yield (QY) of MB and ICG in FBS were calculated by using oxazine 725 in ethylene glycol (QY = 19%) (28) and ICG in dimethylsulfoxide (QY = 13%) (29), respectively, as calibration standards under conditions of matched absorbance (absorbance = 0.08) at 654 nm (MB) or 770 nm (ICG). For injection, MB and ICG were each diluted in 10 ml of saline, with the final dose administered being 0.14 mg/kg and 0.018 mg/kg, respectively. Both were infused as a rapid bolus via a central venous catheter.

FLARE™ Imaging System Components

The newest version of the FLARE™ system permits positioning of the custom optics anywhere in 3-dimensional space, while maintaining a working distance of 18 inches between optics and the surgical field. Light-emitting diodes (LEDs) generate 40,000 Ix of white light (400–650 nm), 4.0 mW/cm² of 670 nm NIR fluorescence excitation light, and 11.0 mW/cm² of 760 nm NIR fluorescence excitation light over a 15 cm field of view. Color video (i.e., the surgical field) and 2 channels (700 nm for MB and 800 nm for ICG) of NIR fluorescence (i.e., fluorescence distribution) images were obtained simultaneously and in real time. Compared to other currently available NIR imaging systems, the FLARE imaging system offers 2 channels of NIR fluorescence, both of which were used in this study. Computer-controlled image acquisition via custom software, color video, and NIR fluorescence images can be displayed individually and/or merged.

Animal Model System

Animals were studied under the supervision of an approved institutional protocol. Six female Yorkshire pigs from E.M. Parsons and Sons, Hadley, MA, averaging 36.1 kg were induced with 4.4 mg/kg intramuscular Telazol, intubated, and maintained with 2% isoflurane. Electrocardiography, heart rate, oxygen saturation, and body temperature were monitored during experiments. A 14-gauge central venous catheter was inserted into the external jugular vein prior to surgery and creation of the nipple sparing mastectomy incisional models. Postsurgically (72 h), the anesthetic procedures were repeated to assess nipple perfusion with the NIR imaging system and another injection was performed at this time. Antibiotics were given twice over a 3-day course as follows: 5 mg/kg of baytril was injected intravenously prior to skin incision and one day postoperatively. Analgesics were given as 0.03 mg/kg of buprenorphine, injected 30 min prior to extubation. Following the injection of buprenorphine, a 75 µg fentanyl patch was placed on the back of each pig.

Surgical Models

Using the FLARE™ imaging system, 4 nipples could be visualized in the same field of view at any given time (Figure 1). The pig has no areola, therefore the incisions were designed with the nipple centered in a 3 cm diameter circle to simulate areolar skin. The first nipple was designated as the control, and received no surgical intervention. The second had a circumareolar incision (3 cm diameter) and preservation of the underlying vasculature, similar to a breast reduction or mastopexy design (Model 1). The third had a periareolar incision (3.5 cm length, Model 2), where extensive undermining was performed and the

underlying vasculature was sacrificed. The fourth had a radial incision (3.5 cm length, Model 3), where similar undermining and sacrifice of the underlying vasculature was performed. The blood supply in these models was presumably from the dermal or subdermal vessels. To eliminate nipple position as a possible confounder, the position of each model was rotated in every subsequent pig.

Quantitative Assessment

Quantitation of fluorescence was described in detail previously.⁽²⁷⁾ Briefly, at each time point, the fluorescence intensity (FI) of a region of interest (ROI) over the nipples and background (BG) intensity in the corner of the image were quantified using custom software. The performance metrics for MB and ICG fluorescence were evaluated with the contrast to background ratio (CBR). $CBR = (FI \text{ of ROI} - BG \text{ intensity})/BG \text{ intensity}$. CBR was measured for 30 s after bolus injection because after 30 s, the CBR curve gradually decreased back to baseline. This assessment was performed to compare all models preoperatively, immediately after surgery at 0 h, and postoperatively at 72 h.

Statistical Analysis

The mean level of CBR was analyzed to compare the models. We used linear contrasts from a linear mixed-effects model, which accounted for the within-pig CBR correlation by modeling the variance-covariance matrix of CBR with a compound symmetry structure. Statistical significance was set at $P < 0.05$. The analyzed values were described as mean \pm SEM.

RESULTS

Optical Properties of MB and ICG

The key optical properties of MB and ICG were measured in 100% FBS. Peak absorbance and emission of MB were found to be 665 nm and 688 nm, respectively. The extinction coefficient at peak absorbance was found to be $71,200 \text{ M}^{-1}\text{cm}^{-1}$. QY in 100% serum was 3.8%. Peak absorbance and emission of ICG were 807 nm and 812 nm, respectively. The extinction coefficient at peak absorbance was $121,000 \text{ M}^{-1}\text{cm}^{-1}$. QY in 100% serum was 9.3%.

Visual Overview and NIR Fluorescence Angiography

Typically, NIR fluorescence appeared at the nipple within 20 s after injection. The preoperative evaluation of fluorescence intensity at the nipple is higher than the surrounding skin and eliminated quickly, suggesting perfusion from a perforator. Throughout this study, there was no total necrosis of the nipple. Two pigs had partial necrosis of the skin around the nipple in the periareolar incision (Model 2). At 0 h, Model 1 (circumareolar) and the control (non-operated) show similar perfusion. However, Model 2 (periareolar) and Model 3 (radial) showed a decrease in the fluorescence intensity of the nipples (Figure 2). At 72 h, Models 2 and 3 showed some recovery of fluorescence intensity; however, the intensity did not return to the preoperative level.

Quantitative Assessment and Statistical Analysis

CBR curves in all models are presented in Figure 3. In the preoperative evaluation, the curves were similar in all models and similar with both MB and ICG showing a peak within 30 s. After 30 sec, both MB and ICG decreased back to their respective baselines. After surgery, some models decreased their maximum value and steepness of the curve. Statistical analysis shows a significant difference between models.

When comparing the 2 fluorophores, ICG and MB show a similar result in their CBR curves. However, the CBR curve of ICG shows more variance than MB. ICG shows model 1 has a higher level of mean CBR than the other models even before surgery (Figure 3). MB could potentially be more reliable for statistical assessment.

At 0 h and 72 h, there was a significant difference between multiple models in MB. Model 1 (pedicled circumareolar) demonstrated similar perfusion to the control model at each time point, although Model 1 had higher perfusion relative to the control model at 0 h. In nipple sparing mastectomy, Model 2 (periareolar) and Model 3 (radial) are used clinically; therefore, our main comparison was Model 2 vs. Model 3. When comparing Model 2 with Model 3, Model 3 had higher perfusion at 72 h ($P < 0.05$), although there was no significant difference at 0 h ($P = 0.148$).

DISCUSSION

In this animal study, nipple perfusion was assessed in 2 nipple sparing mastectomy incisional models. Using near-infrared imaging to measure perfusion, periareolar and radial incisions were compared. There was a significant difference in perfusion at 72 h, as periareolar incisions exhibited decreased perfusion compared to radial incisions ($P < 0.05$). Clinically, there were also 2 cases of partial skin necrosis with the periareolar incision, whereas no necrosis was seen in the radial incisions (see Figure 2). Intraoperative NIR perfusion assessments correlated with clinical necrosis in these 2 cases. This represents the first study to demonstrate differences in perfusion between 2 nipple sparing mastectomy incisions.

Previous reports in the literature have used NIR imaging to assess nipple perfusion. A preliminary study in the literature used ICG as a qualitative assessment of blood supply of the nipple areolar complex after nipple sparing mastectomy (30), evaluating perfusion only at the end of surgery. In the study by De Lorenzi et al., rudimentary quantitative metrics were assessed, multiple incisions were evaluated, and only 9 patients underwent nipple sparing mastectomy. Clinical pilot studies are currently being designed at our institution to correlate with the present findings.

As noted above, several NIR fluorescence imaging systems are available for translation of preclinical results into pilot clinical studies (reviewed in (20)). The differences among these systems are primarily technical. All provide imaging of the otherwise invisible NIR fluorescence, and most provide quantification of results. FLARE™ (31) and mini-FLARE™ (32) also provide 2 independent channels of NIR fluorescence (700 nm and 800 nm) as well as color video overlay.

Both ICG and MB are FDA-approved for other indications and, as shown in this study, can be effective fluorophores for assessment of skin perfusion. Both agents exhibit NIR fluorescence, although the emission peak for each is unique. From this study, MB exhibits less variance than ICG. Because of the decreased variance, MB may potentially be a more effective fluorescent agent to utilize in perfusion assessment. Because the half-life of ICG is much shorter than MB (3.28 to 3.5 min(33) vs. 5.25 h (34)), and ICG is rapidly cleared by the liver after injection, its NIR fluorescence signal was transient and caused larger variance than MB. We found MB to be a more reliable fluorophore to evaluate perfusion at 0 h and 72 h, likely because MB is extracted by the skin and provides a visual surrogate for perfusion. It should be noted that we administered MB as a rapid intravenous bolus, which is not in direct accordance with its present labeling (slow injection over a period of several minutes); however, the dose injected is within dosing guidelines. Although we found no

adverse effects in the animal model, parameters for safe administration of MB need to be established for clinical translation of our results.

We found clear differences among the various models. At 0 h, Model 1 has slightly better blood perfusion than the control model. This paradoxical change is observed only at 0 h. At 72 h, the control model has better perfusion. This demonstrates that pedicle creation, which is commonly performed for a breast reduction or mastopexy, may result in temporary improvements in perfusion after surgery, but equilibrates over time.

Model 1 (pedicled circumareolar) also showed higher perfusion compared to Model 2 (periareolar) or Model 3 (radial). This signifies that preservation of perforators is more important for nipple perfusion than the dermal/subdermal plexus. However, in nipple sparing mastectomy, preservation of the perforating vessels is neither possible, nor oncologically sound. When comparing Model 2 (periareolar) and Model 3 (radial) incisions, there is no difference initially at 0 h. However, at 72 h the linear mixed-effects models revealed significant differences with the radial incision showing higher perfusion ($P < 0.05$).

A limitation of our study is that a pig model was used; therefore, minor anatomical differences between pigs and humans could affect results. For example, the pig has multiple nipples along the torso, which could exhibit variable perfusion. To eliminate this issue, incisional models were rotated from pig to pig. Also, the pig does not have a well-defined areolar border, although this does not appear to affect assessment of perfusion.

In this study, an evaluation was only performed between periareolar and radial incisions; however, newer incisions have been reported in the literature. Regolo et al. reported that a lateral skin incision may be a better incisional selection compared to a periareolar incision due to the absence of visible scars on the anterior breast (16). An evaluation of this new incisional approach is underway, but difficult to create in a pig model.

In clinical practice, it is difficult to accurately compare various incisions, because there are many factors that may also influence perfusion. Komorowski et al. reported that in nipple sparing mastectomy procedures, patient age (especially over age 45) had a significant impact on the risk of necrosis (14). Also, Garwood et al. reported smoking to be a risk factor (18). The reconstructive type may also influence perfusion, as excessive skin tension can result in decreased perfusion (17, 18). Because many factors can influence nipple blood supply in clinical practice, assessment of the correlation between incision and perfusion is often difficult in clinical surgery without large experimental numbers. These factors were eliminated in our animal model, however, future clinical studies will require careful attention to study design.

CONCLUSION

Using the FLARE™ NIR fluorescence imaging system with MB and ICG, we demonstrate in an animal model that radial incisions have higher perfusion over periareolar incisions in nipple sparing mastectomy procedures. Although the optimal clinical choice for incision in nipple sparing mastectomy has still not been determined, our study lays the foundation for future quantitative measurements in patients.

Acknowledgments

Sources of Funding: This study was funded by National Institutes of Health grants #R01-CA-115296 (National Cancer Institute) and #R01-EB-005805 (National Institute of Biomedical Imaging and Bioengineering) to JVF.

This work was funded by NIH grants #R01-CA-115296 and #R01-EB-005805 (JVF). We thank Lindsey Gendall for editing, and Eugenia Trabucchi for administrative assistance.

References

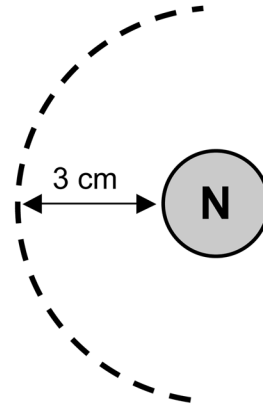
1. Gerber B, Krause A, Reimer T, et al. Skin-sparing mastectomy with conservation of the nipple-areola complex and autologous reconstruction is an oncologically safe procedure. *Ann Surg.* 2003; 238:120–127. [PubMed: 12832974]
2. Petit JY, Veronesi U, Orecchia R, et al. Nipple-sparing mastectomy in association with intraoperative radiotherapy (ELIOT): A new type of mastectomy for breast cancer treatment. *Breast Cancer Res Treat.* 2006; 96:47–51. [PubMed: 16261402]
3. Petit JY, Veronesi U, Orecchia R, et al. Nipple sparing mastectomy with nipple areola intraoperative radiotherapy: one thousand and one cases of a five years experience at the European institute of oncology of Milan (EIO). *Breast Cancer Res Treat.* 2009; 117:333–338. [PubMed: 19152026]
4. Petit JY, Veronesi U, Rey P, et al. Nipple-sparing mastectomy: risk of nipple-areolar recurrences in a series of 579 cases. *Breast Cancer Res Treat.* 2009; 114:97–101. [PubMed: 18360773]
5. Kim HJ, Park EH, Lim WS, et al. Nipple areola skin-sparing mastectomy with immediate transverse rectus abdominis musculocutaneous flap reconstruction is an oncologically safe procedure: a single center study. *Ann Surg.* 2010; 251:493–498. [PubMed: 20134317]
6. Brachtel EF, Rusby JE, Michaelson JS, et al. Occult nipple involvement in breast cancer: clinicopathologic findings in 316 consecutive mastectomy specimens. *J Clin Oncol.* 2009; 27:4948–4954. [PubMed: 19720921]
7. Yueh JH, Houlihan MJ, Slavin SA, et al. Nipple-sparing mastectomy: evaluation of patient satisfaction, aesthetic results, and sensation. *Ann Plast Surg.* 2009; 62:586–590. [PubMed: 19387167]
8. Chen CM, Disa JJ, Sacchini V, et al. Nipple-sparing mastectomy and immediate tissue expander/implant breast reconstruction. *Plast Reconstr Surg.* 2009; 124:1772–1780. [PubMed: 19952633]
9. Djohan R, Gage E, Gatherwright J, et al. Patient satisfaction following nipple-sparing mastectomy and immediate breast reconstruction: an 8-year outcome study. *Plast Reconstr Surg.* 2010; 125:818–829. [PubMed: 20195110]
10. Crowe JP Jr, Kim JA, Yetman R, et al. Nipple-sparing mastectomy: technique and results of 54 procedures. *Arch Surg.* 2004; 139:148–150. [PubMed: 14769571]
11. Schecter AK, Freeman MB, Giri D, et al. Applicability of the nipple-areola complex-sparing mastectomy: a prediction model using mammography to estimate risk of nipple-areola complex involvement in breast cancer patients. *Ann Plast Surg.* 2006; 56:498–504. discussion 504. [PubMed: 16641624]
12. Psaila A, Pozzi M, Barone Adesi L, et al. Nipple sparing mastectomy with immediate breast reconstruction: a short term analysis of our experience. *J Exp Clin Cancer Res.* 2006; 25:309–312. [PubMed: 17167969]
13. Sacchini V, Pinotti JA, Barros AC, et al. Nipple-sparing mastectomy for breast cancer and risk reduction: oncologic or technical problem? *J Am Coll Surg.* 2006; 203:704–714. [PubMed: 17084333]
14. Komorowski AL, Zanini V, Regolo L, et al. Necrotic complications after nipple- and areola-sparing mastectomy. *World J Surg.* 2006; 30:1410–1413. [PubMed: 16850148]
15. Crowe JP, Patrick RJ, Yetman RJ, et al. Nipple-sparing mastectomy update: one hundred forty-nine procedures and clinical outcomes. *Arch Surg.* 2008; 143:1106–1110. discussion 1110. [PubMed: 19015470]
16. Regolo L, Ballardini B, Gallarotti E, et al. Nipple sparing mastectomy: an innovative skin incision for an alternative approach. *Breast.* 2008; 17:8–11. [PubMed: 17870535]
17. Wijayanayagam A, Kumar AS, Foster RD, et al. Optimizing the total skin-sparing mastectomy. *Arch Surg.* 2008; 143:38–45. discussion 45. [PubMed: 18209151]
18. Garwood ER, Moore D, Ewing C, et al. Total skin-sparing mastectomy: complications and local recurrence rates in 2 cohorts of patients. *Ann Surg.* 2009; 249:26–32. [PubMed: 19106672]

19. Rusby JE, Smith BL, Gui GP. Nipple-sparing mastectomy. *Br J Surg*. 2010; 97:305–316. [PubMed: 20101646]
20. Gioux S, Choi HS, Frangioni JV. Image-guided surgery using invisible near-infrared light: fundamentals of clinical translation. *Mol Imaging*. 2010; 9:237–255. [PubMed: 20868625]
21. Matsui A, Lee BT, Winer JH, et al. Image-guided perforator flap design using invisible near-infrared light and validation with x-ray angiography. *Ann Plast Surg*. 2009; 63:327–330. [PubMed: 19692894]
22. Matsui A, Lee BT, Winer JH, et al. Quantitative assessment of perfusion and vascular compromise in perforator flaps using a near-infrared fluorescence-guided imaging system. *Plast Reconstr Surg*. 2009; 124:451–460. [PubMed: 19644259]
23. Matsui A, Lee BT, Winer JH, et al. Submental perforator flap design with a near-infrared fluorescence imaging system: the relationship among number of perforators, flap perfusion, and venous drainage. *Plast Reconstr Surg*. 2009; 124:1098–1104. [PubMed: 19935293]
24. Matsui A, Lee BT, Winer JH, et al. Real-time intraoperative near-infrared fluorescence angiography for perforator identification and flap design. *Plast Reconstr Surg*. 2009; 123:125e–127e.
25. Lee BT, Matsui A, Hutteman M, et al. Intraoperative near-infrared fluorescence imaging in perforator flap reconstruction: current research and early clinical experience. *J Reconstr Microsurg*. 2010; 26:59–65. [PubMed: 20027541]
26. Tanaka E, Chen FY, Flaumenhaft R, et al. Real-time assessment of cardiac perfusion, coronary angiography, and acute intravascular thrombi using dual-channel near-infrared fluorescence imaging. *J Thorac Cardiovasc Surg*. 2009; 138:133–140. [PubMed: 19577070]
27. Matsui A, Tanaka E, Choi HS, et al. Real-time intra-operative near-infrared fluorescence identification of the extrahepatic bile ducts using clinically available contrast agents. *Surgery*. 2010; 148:87–95. [PubMed: 20117813]
28. Sens R, Drexhage KH. Fluorescence quantum yield of oxazine and carbazine laser dyes. *J Luminesc*. 1981; 24:709–712.
29. Benson C, Kues HA. Absorption and fluorescence properties of cyanine dyes. *J Chem Eng Data*. 1977; 22:379–383.
30. De Lorenzi F, Yamaguchi S, Petit JY, et al. Evaluation of skin perfusion after nipple-sparing mastectomy by indocyanine green dye. Preliminary results. *J Exp Clin Cancer Res*. 2005; 24:347–354. [PubMed: 16270520]
31. Troyan SL, Kianzad V, Gibbs-Strauss SL, et al. The FLARE intraoperative near-infrared fluorescence imaging system: a first-in-human clinical trial in breast cancer sentinel lymph node mapping. *Ann Surg Oncol*. 2009; 16:2943–2952. [PubMed: 19582506]
32. Mieog JS, Troyan SL, Hutteman M, et al. Toward Optimization of Imaging System and Lymphatic Tracer for Near-Infrared Fluorescent Sentinel Lymph Node Mapping in Breast Cancer. *Ann Surg Oncol*. 2011
33. He YL, Tanigami H, Ueyama H, et al. Measurement of blood volume using indocyanine green measured with pulse-spectrophotometry: its reproducibility and reliability. *Crit Care Med*. 1998; 26:1446–1451. [PubMed: 9710108]
34. Peter C, Hongwan D, Kupfer A, et al. Pharmacokinetics and organ distribution of intravenous and oral methylene blue. *Eur J Clin Pharmacol*. 2000; 56:247–250. [PubMed: 10952480]

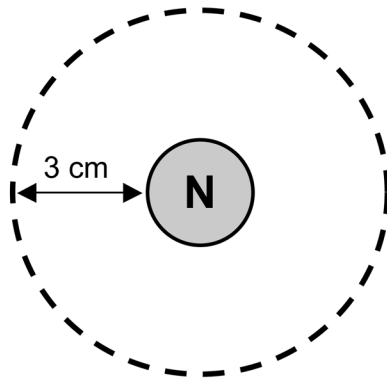
Control
(Non-operated)



Model 2
(Periareolar Incision)



Model 1
(Circumareolar Incision)



Model 3
(Radial Incision)

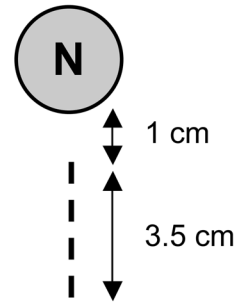


Figure 1. Schematic drawings of the surgical models
Skin incision schemas are shown. Surgery was not performed on the control nipple (N). In Model 1 (pedicle circumareolar), the underlying pedicle and perforators were preserved. In Model 2 (periareolar incision) and Model 3 (radial incision), perforators were dissected and wide undermining was performed.

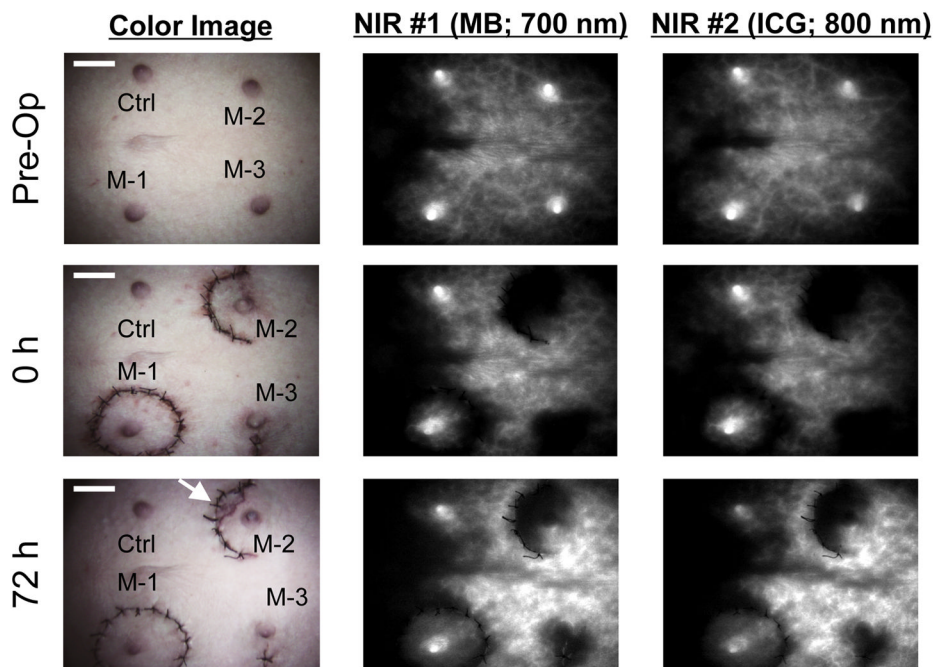


Figure 2. NIR imaging of blood flow, nipple, and skin during the arterial phase of NIR fluorophore administration

10 ml of MB solution (0.14 mg/kg) or 10 ml of ICG (0.018 mg/kg) was injected as a rapid bolus into the external jugular vein. The images are obtained preoperatively (top row), at the end of surgery: 0 h (middle row), and at 72 h (bottom row). At 72 h, Model 2 shows skin necrosis around nipple (arrow). Shown are the color video (left), the 700 nm NIR fluorescence from MB (middle; FLARE NIR channel #1), and the 800 nm NIR fluorescence from ICG (right; FLARE NIR channel #2). Ctrl: Control, M-1: Model 1, M-2: Model 2, M-3: Model 3. Scale bar = 3 cm.

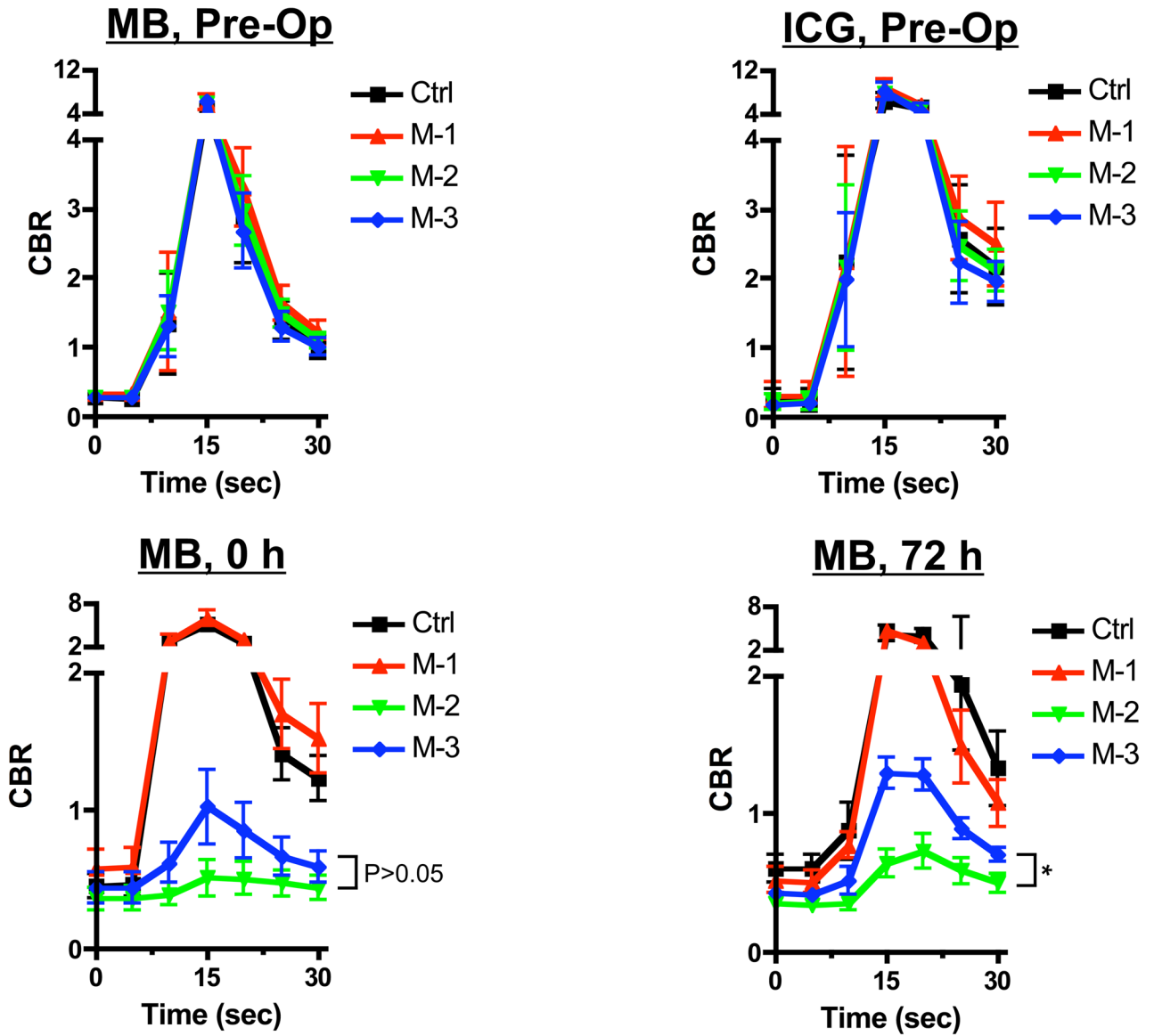


Figure 3. Quantitative assessment of nipple imaging using NIR fluorescence
 Direct comparison of CBR (mean ± SEM) between different fluorophores (MB and ICG) or all models (black line, control; red line, model 1; green line, model 2; and blue line, model 3) using MB (upper left, preoperative; lower left, 0 h; and lower right, 72 h) and ICG (upper right, preoperative). The statistical assessment was from linear mixed effects models with variance-covariance structure of compound symmetry. *P* values for the indicated statistical comparisons are as follows: * = *P* < 0.05.